J Mater Sci (2006) 41:6855–6860
DOI 10.1007/s10853-006-0945-3

Emission spectroscopy analysis for the non-destructive evaluation of the health of thermal barrier coatings

Guofeng Chen · Kang N. Lee · Surendra N. Tewari

Received: 8 September 2005 / Accepted: 6 December 2005 / Published online: 8 October 2006

Abstract Lithium oxide was selected as an emission spectroscopic marker in yttria stabilized zirconia (YSZ) thermal barrier coatings (TBCs). The spectral response of excited lithium atoms from dip-coated YSZ containing 5, 3, 1, and 0.3 wt.% lithium oxide and plasma-sprayed YSZ containing 1 wt% lithium oxide was examined under an oxy-acetylene flame. Results showed that the intensity of lithium emission spectrum is a function of the concentration of lithium oxide in the YSZ, the flame temperature, and the degree of TBC degradation. It indicates that an emission spectroscopy can be used to monitor the degradation of TBCs.

Introduction

Due to the extreme environment it experiences, one gas turbine engine component that most often associated with failure is the thermal barrier coatings (TBCs) on turbine blades [1, 2]. There are four primary components in the TBC system: an yttria stabilized zirconia (YSZ) topcoat, a thermally grown oxide (TGO), an aluminum containing bond coat (BC) and a superalloy substrate. Early detection of TBC degradation and failure is critical to prevent catastrophic engine failure as more advanced gas turbine engines depend on TBCs for their high temperature operation. TBCs on turbine hot section components, therefore, require regular maintenance. A typical maintenance is a visual inspection of the TBC for cracks, erosion or other damages that will indicate the degradation of TBC. These visual inspections require the engine to be taken out of service and to be partially disassembled to provide access to the TBC by boroscope. This type of maintenance is costly because it requires skilled labor and the interruption of service. Therefore, it is desirable to develop a non-intrusive method to detect the failure of TBCs, which is less time-consuming and less expensive compared to the traditional, boroscope examination.

Recently, photo stimulated luminescence spectroscopy has been used to study TBC, which can determine the average biaxial stress of the TGO layer and this information could be used as an indication of incipient failure of TBCs [3–6]. Electrochemical impedance spectroscopy has also been used for the evaluation of TBCs, in which defects such as delamination, spalling, and cracking can be inferred from the changes in the resistance and capacitance on degradation [7, 8]. These two methods are both non-destructive and promising in quality control and remaining life assessment of TBCs. However, neither of them can be used for in situ examination of the failure of TBCs during engine operation. Emission spectroscopy has been used to study the combustion products generated by rocket engines and appears to be promising because of simpler instrumentation, lower cost and availability of considerable emission spectral data [9, 10]. Spectroscopic analysis of the emission from gas turbine

---

G. Chen (✉) · K. N. Lee · S. N. Tewari
Chemical Engineering Department, Cleveland State University, 2121 Euclid Ave, Cleveland, OH 44115, USA
e-mail: gfchen@gmail.com

K. N. Lee
NASA Glenn Research Center, Cleveland, OH 44135, USA

engines could potentially provide valuable information about degradation conditions of TBCs. TBCs can be doped with marker materials that can be optically monitored inside the combustor or in the exhaust. Depending on the mode of TBC failure, marker materials can be incorporated either in the bond coat, in the YSZ top coat or in both. Compositionally graded doping of marker materials is another option. Thus, the detection of the marker species in the combustor or the exhaust would indicate the beginning of TBC failure, and the spectral intensity can be correlated with the extent of coating damages. Lithium oxide (Li_2O) has been evaluated as a potential marker material for environmental barrier coatings [11]. Due to its high emissivity in a wide range of temperatures, little environmental hazard and high melting temperature (1,700 K), lithium oxide (Li_2O) was selected as a marker material for the present work. The purpose of this research was to investigate the potential of emission spectroscopy as a non-destructive evaluation tool to monitor the degradation of TBCs.

Experimental

Slurry dip-coating process was firstly employed to prepare Li_2O-doped YSZ/YSZ two-layer TBC due to its simplicity in preparing the doped YSZ. No bond coat was applied in this preliminary emission test. Lithium oxide was dissolved in water and yttria stabilized zirconia (YSZ: ZrO_2–8 wt.% Y_2O_3) powders (0.8–7.4 μm) were added into the solution and mixed to produce YSZ slurry having 0.3, 1, 3, and 5 wt% lithium oxide. These slurries were used for the preparation of the inner Li_2O-doped YSZ. Polyvinyl butyral (PVB) dissolved into ethanol was mixed with YSZ powder for the preparation of the outer undoped YSZ layer. The inner Li_2O-doped YSZ layer with a thickness of 300 μm was first deposited on CMSX-4 superalloy (nominal composition: 61.7 Ni, 9 Co, 6.5 Cr, 5.6 Al, 1 Ti, 6.5 Ta, 0.6 Mo, 6 W, 3 Re, and 0.1 Hf by wt.%) coupons (disc with 2.54 cm diameter) and dried in a furnace at 100 °C overnight. The outer YSZ with a thickness of 500 μm was coated on these samples, dried at room temperature for 24 h. The TBC-coated superalloy was heated to 500 °C at the rate of 1 °C/min and held at this temperature for 6 h to burn off the PVB in a furnace in air. Air plasma-sprayed YSZ TBCs were also prepared on CMSX-4 superalloy with a Ni–22Cr–10Al–1Y (at.%) bond coat. Plasma-sprayed TBCs have two ceramic layers: an outer YSZ layer and an inner layer of YSZ doped with 1 wt% lithium oxide. Both layers have the same thickness of about 125 μm.

A welder's torch with oxygen and acetylene mixtures was used to obtain flame in order to produce the lithium ions emission spectra. The oxygen and acetylene mixture was controlled to obtain flame temperatures between 1,200–1,800 K. A spectrometer (Model HR2000, Ocean Optics Inc., Dunedin, FL) was installed and configured to cover emission wavelengths from 320 to 800 nm, centered at 670 nm which is the wavelength with the highest Li emission intensity. The emitted light from the lithium ions in the flame travels into an input fiber, which carries the light to the spectrometer. The spectrometer then transmits the information to the PC for data acquisition. A schematic diagram of the spectrometer is illustrated in Fig. 1. The coated coupons were held at one end by an alligator clamp at a 30° angle (a sturdy arrangement) so that the coated surface is exposed directly to the flame and the emitted signals are seen by the spectrometer port [11]. A Pt/Pt–13% Rh thermocouple with its tip placed close to the sample surface was used to record the flame temperature on the specimen surface. However, even with well-controlled flame parameters identical sample surface flame temperature could not be reproduced from one experiment to another. Therefore, the strategy adopted during this research was to measure the surface flame temperature and the corresponding emission signal simultaneously. The emission intensity data was measured when the temperature became nearly constant.

For samples with slurry dipped two-layer TBCs, scratches were machined through the outer YSZ layer to expose the doped inner layer. The dimension of a scratch is roughly 20 mm (length) × 0.3 mm (width) × 0.6 mm (depth). Schematic of the sample is shown in Fig. 2. For the plasma-sprayed TBCs, up to 5 scratches were machined through the outer YSZ layer into the inner doped layer, the width of which was about 1 mm. The scratches simulate cracks. In order to simulate TBC spallation, holes with 1-mm diameter were drilled

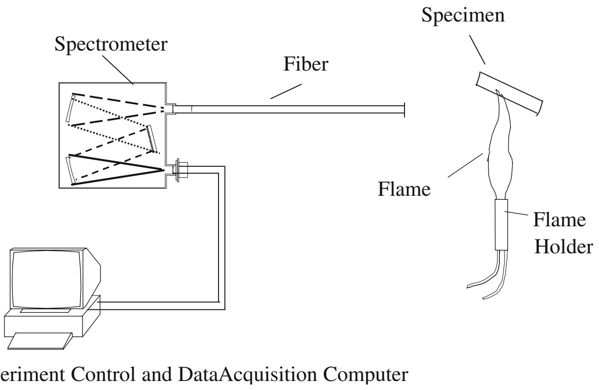

Fig. 1 Schematic diagram of the spectrometer

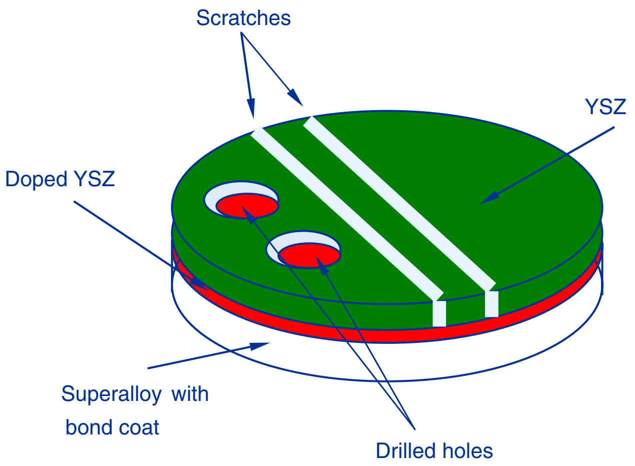

Fig. 2 A schematic representation of slurry dip-coated YSZ TBC

through the outer YSZ layer and into the inner doped layer on the dip-coated YSZ with 1 wt% lithium oxide. All spectra were recorded in a similar lighting condition in the room and the same spectrometer parameters.

Results

Figure 3 illustrates the characteristic luminescence spectrum of lithium ions at its wavelength of 670.8 nm. The intensity used in this study is the value after subtracting the background from the measured. Table 1 lists values of the flame temperature and the corresponding lithium emission intensity for 0.3, 1, 3, and 5 wt.% Li_2O-doped YSZ/YSZ coatings along with their standard deviations. The typical emission intensity (in arbitrary units) versus temperature plot for the slurry dip-processed 1 wt.% Li_2O-doped YSZ/YSZ coating samples is shown in Fig. 4. Error bars in the figure indicate the standard deviation. The “without YSZ outer layer” data represent the complete spallation of the top YSZ TBC layer. In the presence of cracks in the YSZ top layer the portion of the inner doped layer exposed to the flame through cracks is responsible for the excitation of Li atoms. Therefore, increasing the number of scratches simulates increased TBC cracking. Figure 4 shows that the lithium spectral intensity increases with increasing temperature and TBC cracking.

Figure 5 is a plot of emission intensity versus temperature for slurry dip-processed 1 wt.% Li_2O-doped YSZ/YSZ coating having 1-mm diameter holes through the top layer to simulate the coating spallation. As expected the intensity increases with the increasing temperature and the number of holes.

Figure 6 plots the emission intensity for the plasma-sprayed 1 wt.% Li_2O-doped YSZ/YSZ TBCs as a function of sample temperature and the number of scratches. Again, the emission intensity increases with increasing temperature and the number of holes. The emission intensity from the plasma-sprayed TBCs is considerably smaller compared to the slurry dip-coated TBCs even though the scratches were more than twice wider in the plasma-sprayed samples. For example the intensity from the plasma-sprayed TBCs with two scratches is about 60 in an arbitrary unit at 1,370 °C (Fig. 5), whereas the intensity from the dip-coated YSZ with two scratches is about 250 (Fig. 3). This may be due to the different distribution of Li_2O in the two samples. In the plasma-sprayed powders the Li_2O was uniformly distributed within each YSZ particle whereas is concentrated on the surface of YSZ particles in the slurry-dipped process.

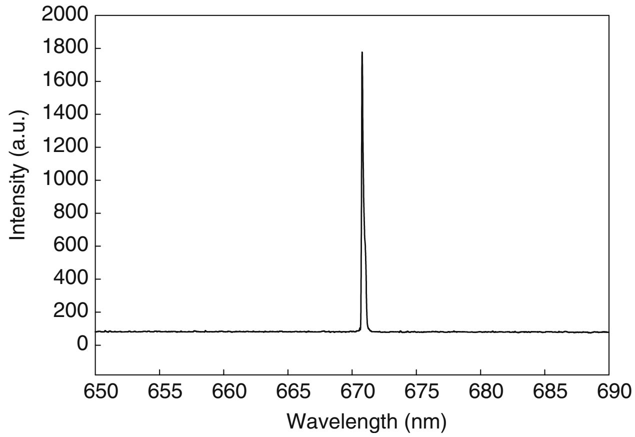

Fig. 3 The characteristic luminescence spectrum of lithium ions at its wavelength of 670.8 nm

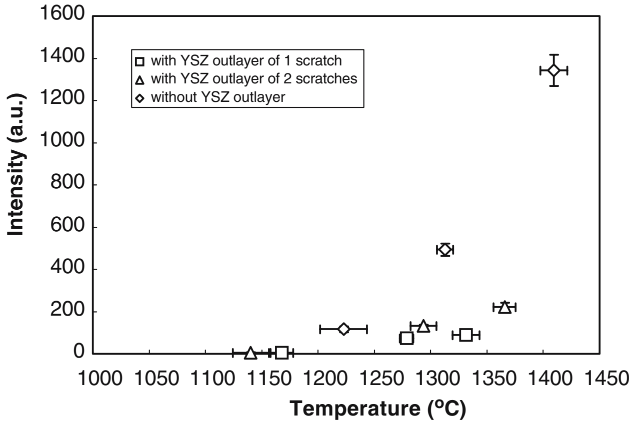

Fig. 4 Effect of flame temperature and dopant concentration on the intensity of slurry dip-processed 1 wt.% Li_2O-doped YSZ

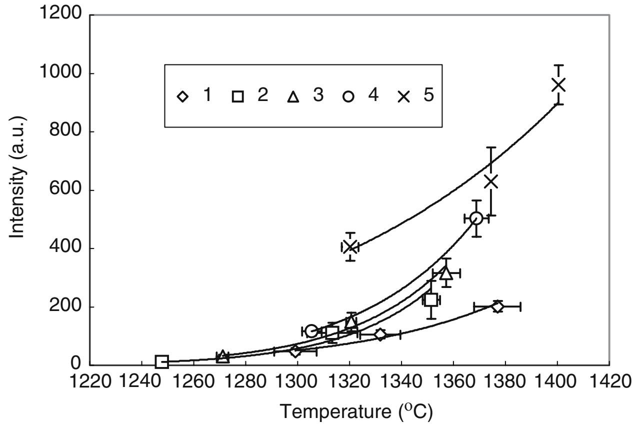

Fig. 5 Effect of flame temperature and number of 1-mm diameter holes on the intensity of slurry dip-processed 1 wt.% Li_2O-doped YSZ/YSZ TBC

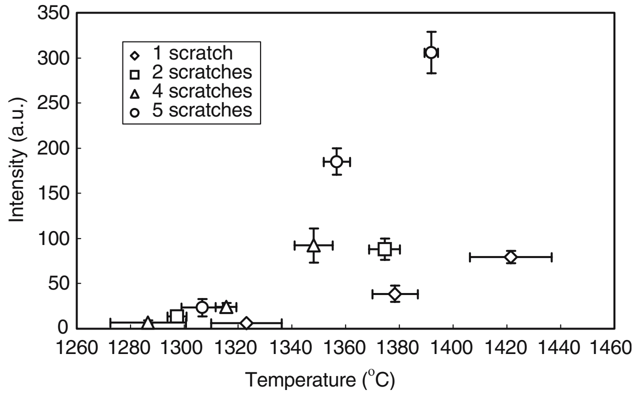

Fig. 6 Effect of flame temperature and number of scratches on the intensity of plasma-sprayed 1 wt.% Li_2O-doped YSZ/YSZ TBC

Discussion

Metal species in flames appear as atomic vapor, metal oxides, or metal hydroxides, depending on the chemical environment created by the fuel/oxidizer [12–13]. Each of these species can be excited by flames to internal energy levels, which are not stable under Boltzmann chemical equilibrium. The internal energy picked up from the excitation source will appear as electronic excitation in atomic species, and as internal vibrational–rotational excitation in oxides and hydroxides. The species equilibrate with their environment by collisional equilibration, resulting in emission radiation. In the present study, lithium atoms excited in high temperature flames emit their characteristic spectral luminescence.

The intensity of the emitted light for the transitions can be given by [12, 13]:

$$I = A_{ij} N_k h(v)\ g_i \mathrm{e}^{(-\Delta E_i/RT)} / Z(T) \qquad (1)$$

where A_{ij} is the transition probability between the initial and final internal energy states, N_k the number density of the species k, $h(v)$ the photon energy, g_i the statistical weight, ΔE_i the transition energy per mole, R the gas constant, T the gas dynamic temperature in K, and $Z(T)$ is the species partition function. For a given atomic species, e.g., lithium, the intensity depends primarily on the concentration (number density) of free lithium atoms in the gaseous phase and the flame temperature. For a constant lithium atom content a plot of ln(I) versus T^{-1} is expected to be linear with the slope representing ΔE_i. The 670.8 nm wavelength lithium line, used in our study, corresponds to the transition of lithium atoms from the 2p to the 2s shell.

Exact measurement of all the sample surface temperatures was not possible during these experiments. Therefore, data similar to those typically shown in Table 1 or plotted in Fig. 3 for the 0.3, 1, 3, and 5 wt.% Li_2O containing slurry-dipped processed YSZ coating samples, having one scratch, were extrapolated (or interpolated) to obtain the emission intensities at 1,200, 1,250, 1,300, and 1,350 °C. From the relationship (1) shown above it is expected that at any temperature the intensity will be directly proportional to the airborne Li atom concentration of the slurry. Assuming a linear relationship between the concentration of Li_2O and airborne Li atom, a plot $I/I_{0.3}$ (observed intensity from any sample/the intensity for the 0.3 wt% Li_2O sample at the same temperature) as a function of Li_2O concentration ratio (i.e., Li_2O concentration/0.3) will give a slope of unity. Figure 7 shows such a plot (the curve can not pass through zero since it sets concentration 0.3 and intensity at 0.3 as reference): the solid line is the linear regression ($r^2 = 0.94$) and the dotted lines indicate 95% confidence interval for the regression. The experimentally observed slope, however, is not unity; it is only 0.15. This indicates, for example, that if the Li_2O content of the slurry is increased three times it causes only a 1.45-fold increase in the observed emission intensity. This indicates that the concentration of airborne Li atom is not proportional to the Li_2O concentration in the doped YSZ.

Data shown in Fig. 7 can now be used to obtain the value of the transition energy, ΔE_i. Experimentally observed intensities at 1,200, 1,250, 1,300, and 1,350 °C for the varying Li_2O concentration samples are first weighted by the above described factor of 0.15, i.e., the observed intensities are divided by $[1 + (0.15 \times C/0.3)]$. This allows us to pool together the intensity data for all the four concentrations in

Table 1 Measured temperature and intensity value for the slurry dip-processed Li_2O doped YSZ/YSZ coating under different conditions

Temperature (°C)			Intensity (a.u.)		
One scratch	Two scratches	No outlayer	One scratch	Two scratches	No outlayer
0.3 wt.% Li_2O					
1202 ± 13	1204 ± 14	1192 ± 9	7.25 ± 1.06	14.3 ± 8.33	59 ± 6.56
1339 ± 8	1298 ± 4	1308 ± 16	73.25 ± 10.47	58.7 ± 5.5	367.7 ± 82.1
1384 ± 12	1393 ± 11	1377 ± 10	85.8 ± 15.28	180.7 ± 21.1	888 ± 56.9
1 wt.% Li_2O					
1168 ± 10	1140 ± 16	1223 ± 21	5.67 ± 2.08	6.33 ± 2.52	117 ± 14.2
1279 ± 6	1293 ± 12	1313 ± 7	74.7 ± 9.45	133 ± 3.6	493 ± 30
1331 ± 12	1366 ± 10	1409 ± 12	90.3 ± 8.02	222.3 ± 19.21	1342.8 ± 73.11
3 wt.% Li_2O					
1099 ± 6	1196 ± 6	1201 ± 13	6.5 ± 3.5	30 ± 11	88.7 ± 16.5
1225 ± 10	1306 ± 27	1298 ± 18	40.7 ± 8.5	234 ± 32	865 ± 82.5
1368 ± 15	1376 ± 9	1387 ± 16	323.3 ± 44.8	438 ± 37.51	1570.7 ± 129.2
5 wt.% Li_2O					
1142 ± 11	1136 ± 41	1031 ± 13	15.7 ± 10.3	28 ± 14.5	132.3 ± 21.03
1126 ± 7	1205 ± 8	1157 ± 12	243.5 ± 31.8	99 ± 2.65	449 ± 140
1362 ± 5	1302 ± 10	1324 ± 14	856 ± 57.9	698 ± 244.6	3818 ± 83.3

order to improve the statistics in determining the temperature dependence of emission intensity, as shown in Fig. 8. Solid line in this figure, a semi-log plot of weighted intensity versus inverse temperature (K^{-1}), indicates the linear regression ($r^2 = 0.99$) and broken lines indicate the 95% confidence interval. The slope yields a ΔE_i value of 288 ± 9 kJ/mol. This value is larger than the literature reported value of the transition energy associated with the 670.8 nm wavelength lithium line, 177.65 k J/mol [12]. One possible explanation for the higher activation energy from this study is the error in the temperature measurement. Thermocouples in flames suffer heat losses due to radiation, conduction, and convection, the magnitude of which increases with temperature. Consequently, the flame temperature determined by thermocouples is always lower than the actual temperature. The disparity between the actual and the measured temperature grows larger at higher temperatures, implying that the slopes in Fig. 8 would be shallower if plotted against the actual temperature.

During engine operations, damage initiation and progression in the form of microcracks can occur in various ways in TBCs, depending on the TBC system.

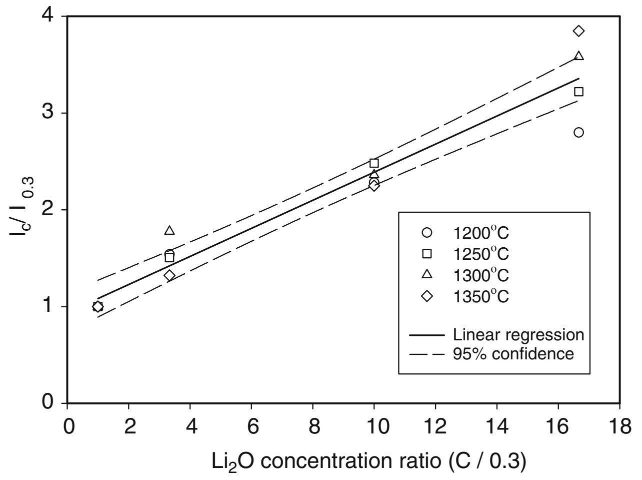

Fig. 7 Relationship between $I_C/I_{0.3}$ (intensity from a coating with C wt.% Li_2O/intensity from 0.3 wt.% Li_2O slurry) and the Li_2O concentration ratio (C/0.3) for slurry dip-processed YSZ coatings with one scratch at several temperatures

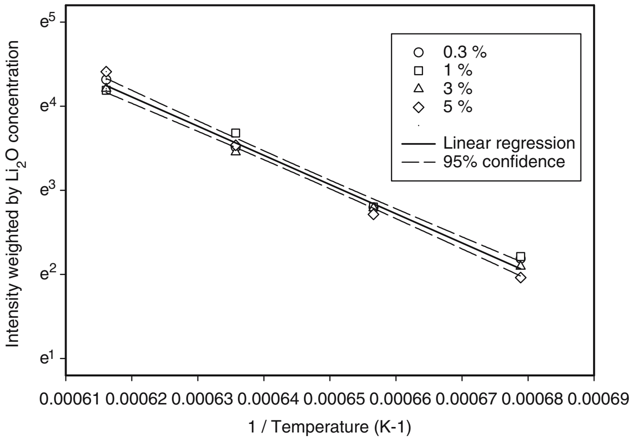

Fig. 8 Temperature dependence of emission intensity. The experimentally determined intensity for 0.3, 1, 3, and 5 wt.% Li_2O doped YSZ/YSZ coated samples have been pooled together to achieve an improved statistics in determining the slope of the intensity versus 1/temperature plot

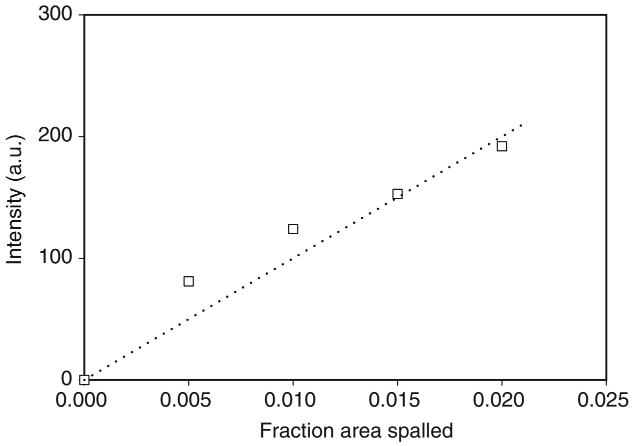

Fig. 9 Emission intensity measured at 1,320 °C versus fraction area spalled (drilled out) for the slurry dip-processed 1-wt.% Li_2O-doped TBCs

Microcracks can develop, propagate and coalescence at the bondcoat/TGO or TGO/topcoat interfaces [1, 2]. The coalescence of the cracks drives the fracture, which can be the source for the vertical or parallel crack initiation within the top ceramic coat. With extended exposure, cracks at the interfaces or within the topcoat lead to the delamination at the interface or through the topcoat, causing the spallation of TBC. In our doped YSZ/YSZ TBC, as the TBC cracks or delaminates, the inner doped YSZ is exposed to the flame and some Li atoms become airborne. The subsequent transitions of Li atoms from the ground state to an excited state and back to a lower energy state cause the radiation of photons having a unique wavelength for each transition. Figure 9 shows such a correlation between the emission intensity (measured at 1,320 °C) and the fraction area spalled for the slurry dip-processed 1 wt% Li_2O-doped TBCs. As mentioned earlier the top YSZ layer was drilled out in these samples in order to expose the bottom Li_2O-doped layer and simulate coating spallation. This figure shows a linear increase in the emission intensity with increasing extent of spallation and demonstrates the viability of using Li emission spectroscopy as a tool to monitor the health of TBCs.

Conclusions

The emission spectral luminescence of lithium oxide-doped YSZ TBC, applied by slurry dip and plasma spraying, was examined. The results showed that the intensity of lithium emission spectrum is a function of the concentration of lithium oxide in the YSZ, the degree of TBC spallation, and the flame temperature. The result demonstrates the emission spectroscopy of lithium oxide doped YSZ inner layer can be used as a non-destructive evaluation tool to monitor the spallation of TBCs in gas turbines.

Acknowledgement This work is supported by DOE UTSR Subcontract No. 03-01-SR106.

References

1. Evans AG, Mumm DR, Hutchinson JW, Meier GH, Pettit FS (2001) Prog Mater Sci 46:505
2. Padture NP, Gell M, Jordan EH (2002) Science 296:280
3. Peng X, Clarke DR (2001) J Am Ceram Soc 83:1165
4. Saunders SRJ, Banks JP, Chen GF, Chunnilall CJ (2004) Mater Sci Forum 461–464:383
5. Nychka JA, Clarke DR, Sridharan S, Jordan EH, Gell M, Lance MJ, Chunnilall CJ, Smith IM, Saunders SRJ, Pillan R, Sergo V, Selcuk A, Atkinson A, Murphy KS (2003) Surf Coat Technol 163:87
6. Sridharan S, Xie L, Jordan EH, Gell M (2004) Surf Coat Technol 179:286
7. Sohn YH, Jayaraj B, Laxman S, Franke B, Byeon JW, Karlsson AM (2004) JOM 56:53
8. Jayaraj B, Desai VH, Lee CK, Sohn YH (2004) Mater Sci Eng A372:278
9. Madzsar GC, Bickford RL, Duncan DB (1992) Proc of the 28th AIAA/ASME/SAE/ASEE joint propulsion conference, Nashville, TN, 6–8 July 1992, pp 1–23
10. Paradis Paul-Francois (1997) 33rd AIAA/ASME/SAE/ASEE joint propulsion conference and exhibit, Seattle, WA, 6–9 July 1997, pp 1–12
11. Ramachandra C, Lee KN, Tewari SN (2004) J Am Ceram Soc 87:1117
12. Alkemade CThJ, Herrmann R (1979) Fundamentals of analytical flame spectroscopy (translated from German by R Auerbach and Paul T Gilbert Jr). Wiley, New York
13. Dean JA, Rains TC (ed) (1969) Flame emission and atomic absorption spectrometry, vol. 1. Mercel Decker, England